DYNAMIC PROGRAMMING BASED MULTICHANNEL IMAGE RESTORATION

Mrityunjay Kumar, Pradeep Ramuhalli

Nondestructive Evaluation Laboratory,
Department of Electrical and Computer Engineering
Michigan State University, East Lansing, MI 48824, USA
{kumarmri, rpradeep}@egr.msu.edu

ABSTRACT

Blind restoration of single-input /multiple-output images finds application in diverse fields including multi-sensor remote sensing, non-destructive testing and medical imaging. In this paper an iterative forward propagation dynamic programming based approach is proposed for restoring images in a single-input/multiple-output multichannel framework. This algorithm exploits cross channel correlation for restoring images, leading to improved performance as compared to single channel restoration. The algorithm is applied to both synthetic as well as experimental data and initial results indicate the feasibility of the proposed algorithm.

1. INTRODUCTION

In many applications of multi-sensor imaging, such as remote sensing, non-destructive testing, medical imaging etc., the measurements obtained from *n* sensors $c_1(x,y),\cdots,c_n(x,y)$ may be modeled as the outputs of *n* linear space-invariant systems (Figure 1) [1]-[3]. If $h_1(x,y),\cdots,h_n(x,y)$ are the impulse responses (or point spread functions, PSF) of these systems, the measurement model is

$$c_i(x,y) = h_i(x,y) * f(x,y),\ i = 1,2,..,N \qquad (1)$$

where $f(x,y)$ is the source object. Since the same source is imaged using different sensors [4], the measured images contain redundant as well as complementary information. Often, measurements in individual channels are distorted versions of the original due to various types of channel/sensor distortions and the goal of multichannel image restoration is to obtain the source from the multiple observations.

Conventionally, this can be done in a single channel framework [2] where only one channel is considered at a time for restoration and there is no information sharing among the channels. However, the quality of the restored image can be improved drastically by taking into account cross channel correlation during restoration. While Wiener filter-based approaches [5] are typically used when the channel parameters are known, in most practical applications the channel parameters are unknown and the source image needs to be estimated based on only the observed images. This is known as multichannel blind deconvolution [6]. In the recent past, probabilistic approaches [7] and total variation [8] based approaches have been proposed for multichannel image restoration. However, these approaches tend to be computationally complex.

An alternative approach is proposed in this paper and is based on the use of dynamic programming methods [9]. An n-channel blind deconvolution problem can be viewed as an $n+1$-dimensional optimization problem where channel parameters as well as the source image are estimated jointly in an optimal manner. However, this approach is challenging because, in general, *n*-dimensional optimization is computationally expensive. The problem is better solved by the use of dynamic programming based approaches as dynamic programming reduces n-dimensional optimization problems to n 1-dimensional optimization problems. At each stage, the Richardson-Lucy blind deconvolution algorithm [10]-[12] is used in thus study to estimate parameters of interest.

The rest of the paper is organized as follows. Section 2 describes the proposed algorithm based on the use of forward propagation dynamic programming. Section 3 presents the results of performance of the algorithm of several databases and finally, Section 4 concludes the paper.

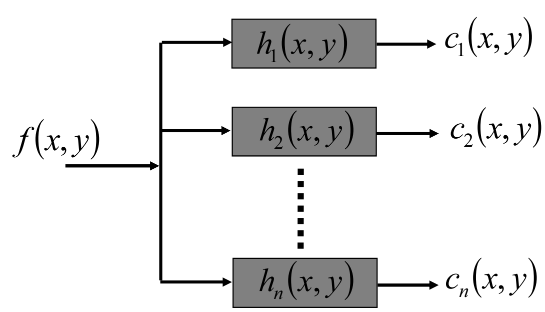

Figure 1. Multichannel measurement model.

2. PROPOSED ALGORITHM

Consider the measurement model in (1), and depicted in Figure 1. Assuming that $f(x,y)$, and $h_i(x,y)$, $i = 1,2,...,N$ are the unknown variables, the problem of estimating them can be expressed in terms of the simultaneous minimization of cost functions P_i, $i = 1,2,...,N$ defined as

$$P_i = \left\| c_i(x,y) - h_i(x,y) * f(x,y) \right\|^2,\ 1 \le i \le N \tag{2}$$

subject to the constraints

$$\begin{aligned} &\sum_{x,y} h_i(x,y) = 1\ \forall i \\ &h_i(x,y) \ge 0,\ i = 1,2,..,N\ \forall\ x,y \end{aligned} \tag{3}$$

This problem can be solved using an *n*-step forward propagation dynamic programming algorithm as shown in Figure 2 where $S_1 \cdots S_n$ are state variables, $R_1 \cdots R_n$ are return functions, $x_1(= h_1)\cdots x_n(= h_n)$ are control variables, $c_1 \cdots c_n$ are constants (observations) and $t_1 \cdots t_n$ are transform functions that estimate the output variables for the different stages respectively. The overall cost function, $P(R_1 \cdots R_n)$, for this model is expressed as

$$P(R_1 \cdots R_n) = \sum_{i=1}^{n} R_i = \sum_{i=1}^{n} \left\| c_i - h_i * f \right\|^2 \tag{4}$$

Clearly, this cost function is monotonic and separable, and therefore, an optimal solution is guranteed if the optimal value of S_1 is known [9]. However, in general, this is unknown, and an iterative approach is necessary for optimization. Thus, the problem can be restated as

$$\underset{\substack{f,h_i \\ 1 \le i \le n}}{Min}\ P(R_1 \cdots R_n) \tag{5}$$

subject to the constraints

$$S_{i+1} = t_i(S_i, x_i) \quad and \quad R_i = r_i(S_i, x_i) \quad i = 1 \cdots n \tag{6}$$

$$\sum_{x,y} h_i(x,y) = 1,\ h_i(x,y) \ge 0,\ \forall i, \forall\ x,y \tag{7}$$

where the values of the state variables are computed iteratively. The complete flow chart for the algorithm is shown in Figure 3. At the k^{th} iteration, the control variable for stage 1 is computed using S_1 estimated at the $(k-1)^{th}$ iteration. The output state variable of stage *i* acts as the input state variable for stage *i*+1. At each stage, the Richardon-Lucy blind deconvolution algorithm [10]-[12] is used to compute the state and control variables. The algorithm terminates when the convergence criterion in (8) is satisfied. Here, η is a pre-defined tolerance value.

$$\left\| f^k - f^{k-1} \right\|^2 \le \eta \tag{8}$$

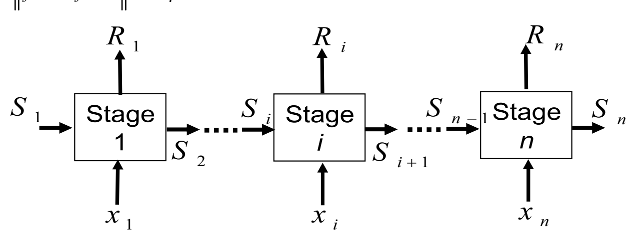

Figure 2. n-stage forward propagation dynamic programming model.

3. RESULTS

The proposed algorithm was tested using multiple databases. The first data set contained benchmark images that were artificially blurred using two known filters (two-channel image restoration). An example is the "cameraman" image in Figure 4 that was blurred using two filters – a low-pass filter h_1 and a high pass filter h_2, where h_1 is a 7x7 averaging filter with pixel value 1 /500 for all the pixels and h_2 is a high pass filter where h_2 = [-1,-1,-1;-1,12.5,-1;-1,-1,-1]/9. The proposed algorithm was used to reconstruct this image and results are presented in Figure 4. Figure 4(a) shows the source image while Figures 4(b) and 4(c) are the outputs of channel 1 and 2 respectively. Multichannel restoration results (Figure 4(f)) are compared with single channel restoration results (Figures 4(d) and 4(e)). The PSF support for single channel restoration is the same as the support of filters used for blurring. For multichannel restoration, two sets of results were computed: one with PSFs for both channels using the same support and the second where different support sizes were assumed. While the results of multichannel restoration are visually pleasing, a quality metric is necessary to objectively compare the two sets of results. The image quality index Q_0 proposed by Wang and Bovik [13] is one of the metrics used to compare the results of different algorithms in this study. This metric compares the restored image with the original image, and a value of $|Q_0| = 1$ indicates that the two images being compared are identical. The greater the deviation of Q_0 from 1, the greater the discrepancy between the two images. Note that this metric can only be computed when the original image is available!

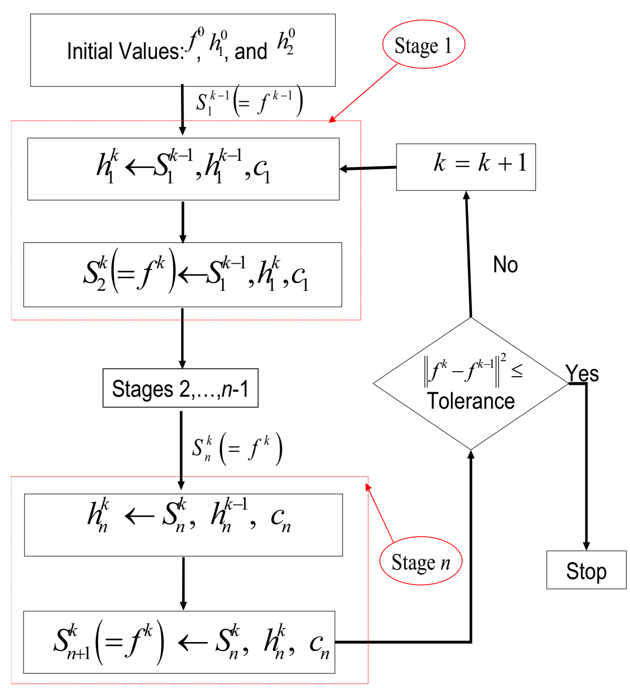

Figure 3. Flow chart of the proposed algorithm

For the results presented in Figure 4, Q_0 for single channel restoration are 0.0101 (Figure 4(d)) and 0.1708 (Figure 4(e)) respectively while Q_0 for the proposed algorithm is 0.4041 (when assuming same size PSFs) and 0.4268 for different size PSFs. It is evident that the results have improved significantly by the use of the multichannel method. Similar results for two other benchmark images are summarized in Table 1. The two channels for the "Lena" image were obtained by applying a motion blur and a Gaussian filter, while two different kinds of motion blur were used to distort the "Text" image.

Results of applying the algorithm in the presence of additive noise indicate that it is robust to noise. Specifically, Q_0 for low SNR (0 dB – 10 dB) for the "cameraman" image were between 0.044 and 0.2174 respectively (same size PSF; 0.1403 and 0.2352 for different PSF sizes), indicating that the reconstructed image has sufficient information for subsequent processing. Similar results were observed with other benchmark images.

The second database consists of measurements obtained by the nondestructive evaluation of Inconel-600 tubing in steam generators in nuclear power plants. Eddy current techniques [14] are used for the inspection of such tubing to detect the presence of cracks. The coil impedance changes in the proximity of flaws, and this fact is used to distinguish regions with flaws. However, eddy current probes tend to have a blurring effect on the true flaw image (Figure 5(a) and 5(b)) due to the fact that the probes are not point probes. Typically, inspection is performed using multiple excitation frequencies, and the measurement (including the blurring effect) can be modeled using a multichannel model similar to that presented in Figure 1.

Determining true flaw dimensions is critical to structural integrity studies, and therefore, the blurring effect of probes must be removed for accurate determination of flaw surface dimensions. Because multiple measurements are carried out at multiple excitation frequencies, multichannel restoration techniques can be used for determining the true flaw dimensions. An example of measurements for a rectangular-shaped notch that is 100% deep (relative to the tube wall thickness) and 0.25" long is shown in Figures 5(a) and 5(b). Single channel reconstruction results and 2-channel reconstruction results are presented in Figures 5(c), 5(d) and 5(e) respectively. Q_0 values for these sets of results cannot be computed, as the true flaw images are not available. However, the length of the flaw is the quantity of interest in this application, and the recovered length of 0.267" from the multichannel algorithm is close to the actual length. This contrasts with the length estimated from the original measurement (0.344"). Note that single channel reconstruction indicates the presence of multiple flaws, and therefore does not allow the calculation of a length.

A summary of results for additional flaw signals is presented in Table 1. These results, in addition to results on other images, are also available online at http://www.msu.edu/user/rpradeep/Publications/Conferences/ICASSP2005/Resuls.html. The results, along with the quality index and visual interpretation, underscore that multichannel reconstruction algorithms are necessary for accurate recovery of the original image, and that the proposed algorithm is capable of accurately recovering the original image from distorted multichannel measurements.

4. CONCLUSIONS AND FUTURE WORK

A multichannel blind deconvolution algorithm based on the use of dynamic programming is proposed in this paper. The algorithm uses the Richardson-Lucy blind deconvolution algorithm in combination with forward propagation dynamic programming to iteratively estimate the original image from multichannel observations. Initial results indicate that the proposed algorithm provides superior performance when compared to single channel blind deconvolution algorithms. The results also indicate that the algorithm is robust to additive noise.

5. REFERENCES

[1] A. K. Jain, "Advances in mathematical models for image processing," *Proc. IEEE*, vol. 69, No. 5, pp. 502-528, 1981.

[2] H. C. Andrews and B. R. Hunt, *Digital Image Restoration*, Prentice-Hall, Englewood Cliffs, NJ, 977.

[3] C. A. Berenstein and E. V. Patrick, "Exact deconvolution for multiple convolution operators — An overview plus performance characterizations for imaging sensors," *Proc. IEEE*, vol. 78, pp. 723–734, 1990.

[4] D. Hall, *Mathematical Techniques in Multisensor Data Fusion*, Boston, MA: Artech House, 1992.

[5] N. P. Galatsanos and R. T. Chin, "Digital restoration of multichannel images," *IEEE Trans. Acoust., Speech, Signal Processing*, vol. 37, no. 3, pp. 415–421, 1989.

[6] G. B. Giannakis, R. W. Heath, "Blind Identification of Multichannel FIR Blurs and Perfect Image Restoration," *IEEE Trans. Image Processing*, Vol. 9, No. 11, 2000.

[7] B. C. S. Tom, K. T. Lay, and A. K. Katsaggelos, "Multi-channel image identification and restoration using the expectation-maximization algorithm," *Opt. Eng.,* vol. 35, pp. 241–254, 1996.

[8] P. V. Blomgren, "Total Variation Methods for Restoration of Vector Valued Images," *Ph.D. dissertation*, Univ. California, 1998.

[9] D. A. Pierre, *Optimization Theory With Applications*, Dover Publications, Inc., New York, 1986, pp. 367-418

[10] W. H. Richardson, "Bayesian-based iterative method of image restoration," *J. Opt. Soc. Amer. A*, vol. 62, No. 1, pp 55-59, 1972.

[11] L. B. Lucy, "An iterative technique for the rectification of observed distributions," *The Astronomical J.*, vol.79, No. 6, 745-754, 1974.

[12] G. R. Ayers and J. C. Dainty, "Iterative blind deconvolution method and its applications," *Opt. Lett.*, vol. 13, pp. 547–549, 1988.

[13] Z. Wang and A. C. Bovik, "A universal image quality index," *IEEE Signal Processing Letters*, vol. 9, No. 3, pp. 81–84, 2002.

[14] P. Ramuhalli, and S. Udpa, "Automated analysis of rotating probe eddy current data", *Technical Report, EPRI* (1007866), Palo Alto, CA, 2003

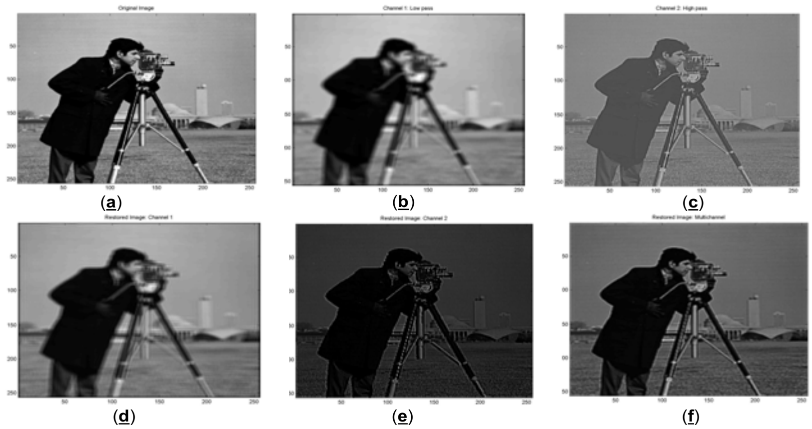

Figure 4. (a): Original Image, (b): Output of channel 1, (c) Output of channel 2, (d): Restored image using channel 1 only, (e): Restored image using channel 2 only, and (f) Output of the proposed algorithm

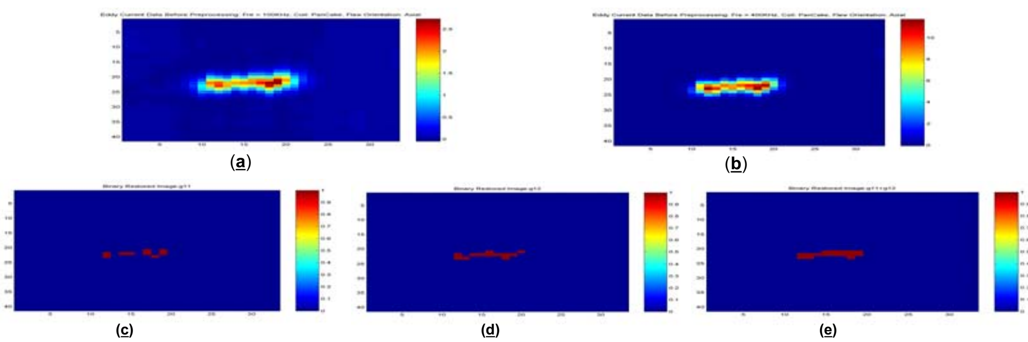

Figure 5. 100% axial EDM notch (a) Channel 1 C-scan image (b) Channel 2 C-scan image at (c) Restored image from channel 1 only (d) Restored image from channel 2 only (e) Multichannel image restoration.

Table 1. Performance summary of the proposed algorithm on several different data sets.

Benchmark Images							
		Quality Index					
	Images	Channel 1 Reconstruction	Channel 2 Reconstruction	Same size PSF: PSF Sizes	Same size PSF: Multichannel Reconstruction	Different size PSF: PSF sizes	Different size PSF: Multichannel Reconstruction
1	Cameraman	0.0101	0.1708	3x3 and 3x3	0.4041	5x7 and 3x3	0.4268
2	Lena	0.4211	0.3920	9x9 and 9x9	0.4885	7x7 and 7x15	0.6029
3	Text	0.8701	0.8459	5x5 and 5x5	0.7258	5x11 and 7x11	0.8108
Eddy Current Inspection Data							
	EDM Notch Type	Flaw Length Estimated from measurement	Flaw Length (True Flaw Length)				
1	100% Axial	0.344”	–	–		0.2670” (0.250”)	
2	100% Circ	0.330”	–	–		0.2370” (0.250”)	
3	20% Axial	–	–	0.2670” (0.250”)		0.2670” (0.250”)	
4	59% Circ	–	–	–		0.2370” (0.250”)	